Shahrood University of Technology
Iranian Society of Mining Engineering (IRSME)
Journal of Mining and Environment (JME)
journal homepage: www.jme.shahroodut.ac.ir
THOMSON REUTERS

Estimation of Pb and Zn Elements using Adaptive Neuro-Fuzzy Inference System (Case study: Gerde Kooh area, north of Yazd)

Shahou Rezaei* and Ali Imamalipour

Department of Mining Engineering, Urmia University, Urmia, Iran

Article Info

Received 2 January 2022
Received in Revised form 3 June 2022
Accepted 19 June 2022
Published online 19 June 2022

DOI:10.22044/jme.2022.11540.2140

Keywords

Earth Sciences
ANFIS-SCM
Lead and Zinc Elements
North of Yazd

Abstract

In the recent years, according to the difficulty of accurately measuring parameters and demarcation of earth sciences, attempts have been made to simplify the natural events for better investigation using geo-modelling. Modeling with intelligent methods is one of the new methods that has been considered in this field in the recent years. In this work, the intelligent method of adaptive neural-fuzzy inference system (ANFIS) is used to predict the elements of lead and zinc located in the Guard Kooh area, north of Yazd province in Iran. Descriptive statistics of data and correlation matrices of studied elements are obtained using the SPSS software. After the data is standardized, imported to the MATLAB software, and the lead and zinc elements are predicted using the ANFIS-SCM method. In this method, 70% of the data (175 samples) are set as the training data, and the rest (75 samples) are set as the test data, which are randomly selected. Using the obtained results, it is found that the grade of the estimated elements in the studied area has a good accuracy and a high correlation with the grade of the analyzed elements. As a result, the ANFIS-SCM intelligent method is a useful and accurate method for estimating the lead and zinc elements.

1. Introduction

A large volume of industrial raw materials is minerals, which due to excessive consumption of raw materials in the recent years, many industries have faced difficulties in supplying their raw materials. Minerals have also been transformed from high-grade and available materials to low-grade minerals with limited availability due to high consumption in the recent years.

According to studies, the soils of Iran have low zinc concentration, and therefore, most people in this country are deficient in zinc in their bodies [1].

Traditional methods in the science of mineral exploration, in addition to limited capability, cost a lot of time and money. In the recent years, the human beings have resorted to using methods that have achieved the most results with less cost and time. Earth sciences are among the sciences in which many factors are involved in shaping the results. Therefore, instead of trying to surround all the factors involved, creating an appropriate model that generally reflects the states and relationships between these factors, eliminates our need to analyze how minerals are formed. Therefore, modeling in earth sciences has gained a special importance. On the other hand, due to the problems and limitations of sampling in earth sciences, the traditional modeling methods that require a large amount of data are less efficient [2].

Of course, it is necessary to mention that the modeling methods are used as an auxiliary method in any science, and their use is done along with study and research, and finally, a definite result according to the opinion of the expert. Modeling with intelligent methods follows the same rule, and it is necessary to examine the relationship between different inputs with outputs, numbers, and other parameters in each step as an expert. In general, this method, like other methods, should be considered a tool, and its efficiency depends on how it is used.

* Corresponding author: shahou44@gmail.com (S. Rezaei).

Intelligent methods have been used in different sciences for different purposes. In general, in problems where the right amount of data is available, by selecting the appropriate inputs and outputs for model training, it is possible to model the desired range. Of course, the intelligent methods are generally combined for different problems, and by comparing their results, the optimal method can be selected [2].

Numerous studies have been conducted on the application of intelligent methods in the earth sciences, among which the following studies can be mentioned: Skabar (2003) using artificial feed neural network, mineral potential map in southwest Victoria, Australia prepared gold exploration. The input variables used included the geological, geophysical, and geochemical data of the region. The potential map obtained from this study was significantly improved compared to the previous studies using the traditional methods [3]. In another study, Fung *et al*. (2005) have compared different artificial neural networks to determine the mineral potential.

Four different artificial neural networks, polynomial artificial neural networks, general regression artificial neural networks, probabilistic artificial neural networks, and post-diffusion artificial neural networks were compared. When the output interval value was 0, it was considered that the general regression artificial neural network had the highest efficiency, and the polynomial artificial neural networks had the lowest efficiency. Finally, the researchers suggested that the optimization algorithms such as genetic algorithms and fuzzy logic be used when conflicting results are obtained from different networks [4].

In another study, Leit and Filho (2009) have used probabilistic artificial neural networks to map the potential of platinum group elements in the Karajas region of Brazil. Two potential maps were drawn, one of the potential of gold and platinum group elements and the other for copper and platinum group elements. Gold potential map and platinum group elements with three classifications of the high, medium, and low potential areas; and the potential map of copper and platinum elements group were prepared by two classifications of high and low potential areas. In the gold potential map and platinum group elements, 0.57% of the studied area had a high potential and in the copper potential map and platinum group elements, 0.17% of the areas had a high potential [5]. In another study, Wang *et al*. (2011) using the data from geological maps, geological sections, exploratory boreholes, gravimetry, and magnetometry, and using methods of the fractal, multiple fractals, and probabilistic artificial neural networks obtained a 3D geological model of the molybdenum, lead, zinc, and silver porphyry deposits in the Lanchan region of China. In this study, the application of an artificial neural model was used to accumulate layers of various anomalies including geological and geochemical anomalies [6].

In one study, Twarakavi *et al*. (2006) have prepared a spatial distribution map of arsenic in a gold mine using a support vector machine and at least-squares of an advanced support vector machine. The analysis showed the results of a higher efficiency and a better predictability of the support vector machine and at least-squares of the strong support vector machine compared to the artificial neural network and kriging methods. The performance of the support vector machine was affected by remote points. Removing remote points from the dataset and using a backup vector machine improved the results [7]. In another study, Abedi *et al*. (2012) have performed a multi-classification of the mineral potential areas of Nochun porphyry copper located in the Kerman province of Iran using a support vector machine. The support vector machine method, which is a data-driven method of pattern recognition, divided twenty-one boreholes into five classes with a classification accuracy of 52.38% [8].

In another study, Robinson (2000) has used the fuzzy logic method to determine the potential of a mineral area. Conventional methods classified the mineral potential of the region into two classes, high potential, and low potential. With this method, they also studied the fuzzy logic of vector areas with the medium's potential. The data and information layers were combined in the GIS environment [9].

In another study, Abedi *et al*. (2013) have used a hierarchical fuzzy logic method to determine the potential of a porphyry copper deposit. Several geophysical data obtained from magnetometric and electrical methods were used for this purpose. Three weights, experts were used to weigh the layers of information, and the classification based on mineral potential was made using the fuzzy logic method. The determination of the accuracy and validity of the results was also examined using existing drilling results, which showed promising results [10]. In another study, Tahmasebi and Hezarkhani (2012) have introduced a new method for grade estimation. This method was based on an artificial neural network and fuzzy logic, which was called an emergency neural-fuzzy inference system, which was a combination of two methods,

artificial neural network and fuzzy logic. The combination of these two methods of artificial intelligence is achieved through the verbal and numerical power of intelligent systems. In order to improve the efficiency of this system, a genetic algorithm was used as a known method to solve the complex optimization problems to optimize the network parameters such as learning rate, network movement, and the number of membership functions for each input. The comparison of these methods (artificial neural network, adaptive neural-fuzzy inference system) with this new method was done through a case study in the Songun copper mine, located in East Azerbaijan, Iran. The results showed that the new method could be a faster and more accurate alternative to the existing time-consuming methods for grade estimation. Therefore, its use was suggested for estimating grades in similar problems [11]. In another study, Ziaee *et al*. (2007) have used a combination of the artificial post-diffusion neural network model and vertical geochemical zoning to separate the hidden ore from the dispersed mineral area. With the results obtained from the proposed model and exploratory drilling in the area and the presence of porphyry copper deposits, the efficiency of this model was confirmed [12].

Renguang Zuo *et al*. (2021) have interpreted and visualized geochemical exploration data using the GIS and machine learning methods. Although various methods such as classical statistics, multivariate statistics, geostatistics, fractal/multifractal models, and machine learning algorithms have been successfully used to process geochemical exploration data, the efficient interpretation and visualization of geo-chemical exploration data still support reservoir exploration. It is provocative. In this study, a study for intelligent interpretation and visualization of geochemical exploration data, defined as the processing of geo-chemical survey data with the support of a Geographic Information System (GIS) and machine learning algorithms was proposed in the Sichuan Province, China [13]. Tahmoursi *et al*. (2021) have intelligently modeled geo-chemical exploration using a multi-class support vector machine and have integrated it with a continuous genetic algorithm in the Gonabad region, Khorasan Razavi, Iran. The results of this study showed that these methods could be used for intelligent mineral exploration and subsequent determination of mineralization zones. The above algorithms are applied to avoid wasting time and work, and in cases where the sampling result cannot be determined directly [14]. Renguang Zuo *et al*. (2021) have dealt with the methods of processing geo-chemical exploration data: past, present, and future. In this study, we review common methods for processing geo-chemical exploration data and identifying geo-chemical anomalies associated with mineralization. The results showed that in the future, deep learning algorithms will become a popular technique for geo-chemical data exploration and mining-related mining purposes in mineral exploration [15]. Guopeng Wu *et al*. (2021) have studied unsupervised machine learning for lithological mapping using geo-chemical data in areas covered by Jining, China. This study highlights the ability of unsupervised learning to map intelligent lithology in the covered areas using the geo-chemical data of major stream sediments [16]. Bao-yi Zhang *et al*. (2021) have devised machine learning strategies for classifying rock stratigraphy based on geo-chemical sampling data (a case study in the Chahanwusu River District, Qinghai Province). Classification of rock stratigraphy is possible through the concentration of geo-chemical elements in sediments, and the XGB and LGBM algorithms are recommended for rock stratigraphy classification [17]. Ghadiyanloo *et al*. (2021) have identified the goals of porphyry copper mineralization in the Chahar Gonbad region of the Kerman province using the intelligent method of extreme learning. The evaluation of the models showed that the areas with high copper mineralization potential, which had been identified as exploratory targets, were in good agreement with the known copper events as well as with the characteristics of the geological index. Therefore, the goals can be planned for further exploration programs [18].

Since limited studies have been performed using the intelligent methods to investigate the grade of lead and zinc elements in the Gerde Kooh area, north of Yazd, this study, to predict the grade of lead and zinc elements in this area, using the method of adaptive neural-fuzzy inference system (ANFIS) is discussed.

2. Study and Sampling Area

The studied area is located in the north of Mehdiabad lead and zinc mine in Yazd and 70 km SE of the Yazd city and the closest residential area to the area is Gerde Kooh village, which is located 25 km west of it. The area to be explored, located in the SE corner of the 1:100,000 Fahraj sheet, includes the 11-sided ABCDEFGHIJK with an area of 10 square kilometers, the coordinates of which are given in Table 1.

Table 1. Coordinates of studied area.

UTM, WGS84, Zone 40					
No.	**X**	**Y**	**No.**	X	Y
A	299050.2	3498675	G	305732.2	3495268.2
B	300749.6	3498675	H	305594.4	3495210.8
C	300745.8	3498374	I	304252.4	349465.4
D	301857.9	3498371.5	J	301584.9	3496202.2
E	301875.7	3497080	K	299980	349848.2
F	305873.7	3497079.7			

The studied area is located on a series of mountains containing the lead and zinc mine of Mehdiabad, Yazd, and about half of the area consists of heights and the other half consists of alluvial plains and low hills. These heights are exposed as mountain ranges with a general trend northwest-southeast. These outcrops are composed of Cretaceous rocks below the Taft Formation, which due to erosion, faulting and folding, have formed stigmatic heights and are sometimes difficult to cross. These heights are located in the central parts of the area. The parts around these heights are composed of a sedimentary sequence of Sangestan formation, which is characterized by special marl erosion and drainage network of dendritic waterways and has a milder topography than the other parts. Due to the presence of calcareous layers in the series of detrital rocks of the Sangestan formation and the hardness of these rocks than the detrital layers, these layers have appeared in a stepped manner on the slope. The difference in height between the highest point and the lowest point is in the range of about 400 m [19].

3. Geology

The studied area is located in the SE corner of the 1:100,000 Fahraj sheet. The Fahraj map is located in the southern part of the structural zone of Central Iran but due to the trend of outcrops and structural elements, which show the northwest-southeast and the approximate proximity to the Sanandaj-Sirjan structural zone, this area may be the impact of the Zagros Mountains.

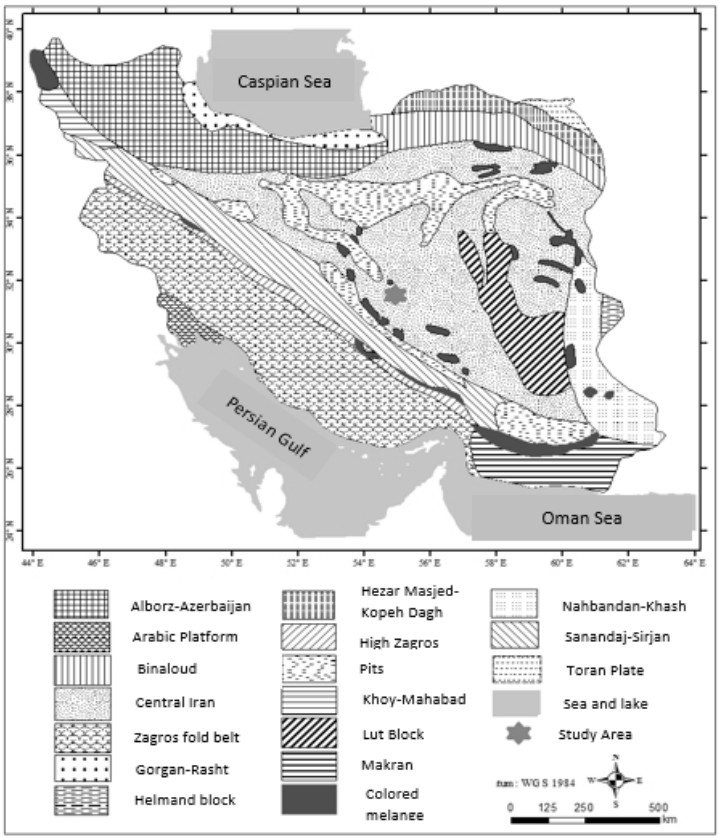

Figure 1. Location of studied area on structural division map of Iran [19].

In order to identify the rock units and also to investigate the possible presence of mineralization in different sections, an area of 10 square kilometers was identified to prepare a mineral geological map with a scale of 1:5,000. Therefore, by conducting field surveys, the rock units were sampled and mineralized, and also the boundaries of stratigraphic and fault units were collected using manual GPS. In this regard, a total of 12 samples were taken from 8 thin section samples, and from 4 samples (mineralization and alteration) thin-polished section was prepared, which are described below.

3.1. Stratigraphic rock units

Based on field surveys and petrographic studies performed on the samples taken in the 1:5,000 mineral geological map, the exposed rock units in the area are divided into two main groups. These two groups include Lower Cretaceous sedimentary units and Quaternary sediments.

3.1.1. Lower Cretaceous sedimentary units
3.1.2. Quaternary sediments

Lower Cretaceous rocks exposed in this area include two formations, Sangestan and Taft. The units of the Sangestan formation consist of brown sandstones below and thin layers of shale, sandstone, siltstone, and olive-green marl limestones. They are greenish-grey, and are exposed in low sections. The units of the Taft formation are mainly composed of limestone and dolomitic limestone with nodes and chert bands. This formation has formed the high and steep parts of the region. Quaternary units in the region also mainly consist of young and old alluvial garrisons and stream sediments.

3.1.1.1. Sangestan Formation

The units of this formation are the oldest stratigraphic rock units exposed in the area and are mainly exposed in the eastern, northeastern, and southern parts. This formation itself consists of two separable units in the desired scale, which are discussed below.

A) K_s^s Unit

This unit is the oldest stratigraphic unit in the area to be explored and consists of a sandstone unit with a thickness of about 400 m consisting of red to brown and gray archetypal sandstones. It is seen in dark gray to brown desert color.

B) K_s^{sh} Unit

The rocks of this unit have an outcrop on the unit and consist of a period of silty-marl limestone, sandstone, shale, and siltstone in olive green to grayish-green desert colors. This unit is manifested in the form of eroded outcrops and sometimes in the form of marl erosion.

The layers of this unit have a general trend of northwest-southeast and have a slope of about 15 to 30 degrees to the west-southwest and in some parts, there are wrinkles. This unit is visible only in the northeastern half and in the southwestern half, it has gone under the sandstones of the Sangestan formation by a large normal fault. The border of this unit with the lower and upper units is gradual and continuous. The average thickness of this unit is about 90 m.

3.1.1.2. Taft formation

Taft formation in this area consists of two units, the lower unit has a continuous border with the upper unit of the Sangestan Formation.

The youngest exposed rock unit in the area also consists of dolomitic rock-forming limestones that have created difficult-to-cross heights.

A) K_t^{l2} unit

This unit is continuously located on the green limestone-marl unit of Sangestan formation in the explored area and its distinguishing feature is the color, type of erosion, and nap bands. The mentioned unit consists of alternating from thin to medium layers of limestone and dolomitic limestone in gray to cream color. Has been.

B) K_t^{l1} unit

This unit has formed the youngest rock outcrops in the studied area, and is composed of cream to light gray dolomitic reef-karst limestones that due to the presence of numerous karsts in the desert facade in the form of honeycombs has appeared. No special layering is observed in them, and it is more visible in the form of masses.

Its border with its lower unit is quite significant in most parts but in some parts, it can be seen gradually and continuously with unit $Ktl2$.

This unit is located in the southeastern part due to the operation of a large normal fault, next to the lower unit of the Sangestan formation (Kss).

3.1.2. Quaternary units

Quaternary units in the area, referred to as young deposits, actually include alluvial plains, river sediments, debris, and rock blocks that have fallen

on the slopes. In the following, the mentioned units are described separately.

A) Q_t^1 unit

This unit consists of alluvial barracks consisting of old unhardened sediments, which with relatively horizontal layering extend only in a few small parts of the studied area, and are mainly deposited in the higher parts of the plains.

B) Q^{t2} unit

This unit includes young alluvial barracks and floodplains that are spread in the lower parts of the plain and consists of unhardened layers and clay and silty sediments that cover a large part of the studied area, and include parts with different sizes are older units.

C) Q^{al} unit

This unit consists of the present-day river sediments, and consists of a collection of detached sediments to gravel along with soil and gravel particles from river streams within large and small waterways of the region. They have an outlook.

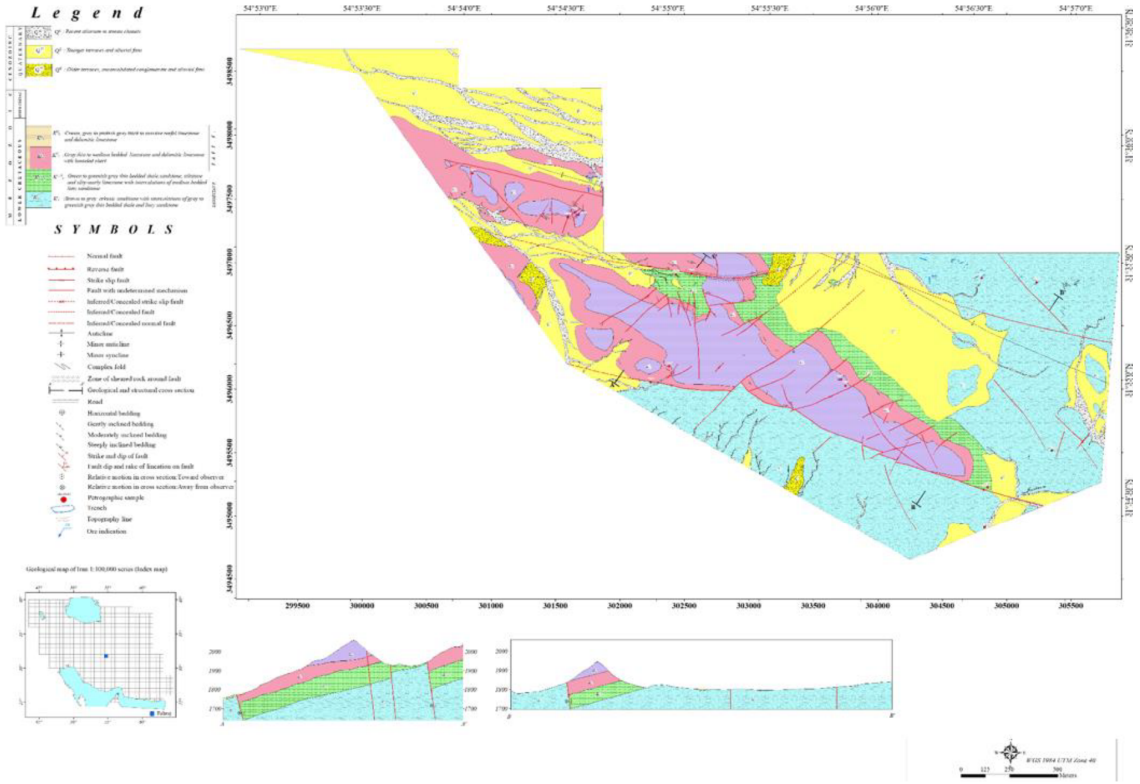

Figure 2. Mineral-structural geological map 1:5000 area.

4. Mineralization in Studied Area

Mineralization occurs in two parts, one is silicate mineralization on the openings and karst cavities of dolomitic limestones of Taft formation and the other is part mineralization with gallons inside sandstone and shale Sangestan and Taft formations.

5. Alteration

Among the observed alterations in the studied area are dolomitization and silicification. The process of dolomitization in the Taft formation is abundantly visible and the effect of this process has created caves and karst cavities.

Another alteration seen in this range is iron oxide and hydroxide alteration, which is affected by the performance of ferrule waters, anchorite dolomites, and forms an iron-rich zone. This iron-rich reddish-yellow area is mainly found in fault zones. This alteration is not very large, and its intensity is very weak.

6. Field Operations, Geochemical Sampling, and Chemical Analysis

In this area, about 20 samples were designed and collected per square kilometer. The sampling network is less located in the main basins, and the location of the samples is closer to the tributaries

of waterways. Except for the above, it has been tried to have approximately the same distribution of geo-chemical samples. The weight of the sample was about 300 g to 500 g, which was collected using an 80-mesh sieve. In total, 250 geo-chemical samples have been collected in this project.

The samples are taken after initial homogenization at a weight of about 20 g for analysis of samples by the ICP method. In the geo-chemical exploration plan of the studied area, the geo-chemical samples were transferred to the Zarazma Company for analysis.

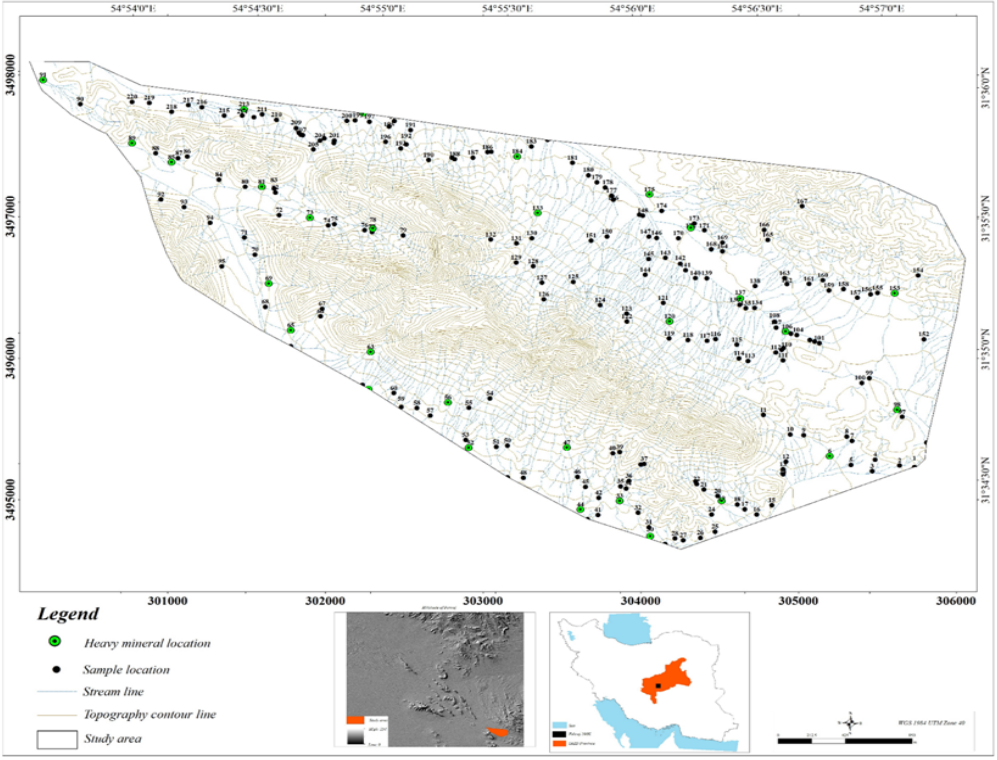

Figure 3. Location of samples taken.

7. Analysis of Comparative Neural-Fuzzy Inference System (ANFIS) Method

The combination of the fuzzy logic and artificial neural networks leads to the creation of a fuzzy neural system that has the advantages of both fuzzy systems and artificial neural networks [20, 21]. In other words, a fuzzy neural system is a fuzzy system that uses a training instruction processed from a training algorithm derived from or inspired by the artificial neural network theory to determine its parameters (fuzzy sets and rules). The function of neural networks is directly related to the number and quantity of educational data [22], so when the number of educational data is small, the results of artificial neural networks are not very reliable. In such cases, the combination of artificial neural networks and fuzzy logic improves the performance of the artificial neural network system and acceptable results [23].

The neural fuzzy adaptive inference system was introduced, a fuzzy inference system whose membership function parameters are modified by the post-diffusion method alone or in combination with the least-squares method [24]. In this research work, an ANFIS model has been used to identify the membership functions, which is: reduction clustering method, which is provided in the following brief description of this model.

7.1. Decreasing clustering

The reduction clustering method has been proposed by Chiu [25], where the data is considered the candidates for the cluster center. This method is as follows:

First, a set of n data points $\{X_1, X_2, X_3, ..., X_n\}$ in the next M space is considered. Since each data is a candidate for the cluster center, the density measurement X_i is defined at the following point:

$$D_i = \sum_{j=1}^{n} \exp\left(-\frac{\left\| x_i - x_j \right\|^2}{\left(\frac{r_a}{2} \right)^2} \right) \quad (1)$$

where r_a is a positive constant. A data point will reach a high density if there are many points in the neighborhood. Defines the r_a radius of a neighborhood; The data points outside this radius are of little help in measuring the density. After measuring the density of each data point, the data point with the highest density measurement is selected as the center of the first cluster. If X_{c1} is the point selected and D_{c1} measured its density, the density measurements for each data point are as follows:

$$D_i = D_i - D_{ci} \exp\left(-\frac{\left\| x_i - x_{ci} \right\|^2}{\left(\frac{r_b}{2} \right)^2} \right) \quad (2)$$

where r_b is a positive constant. After calculating the density for each data point, it was revised, X_{c2} was selected in the next cluster center, and all density calculations for the data were revised. This process continued as long as it produced a sufficient number of cluster centers. The reduction clustering algorithm is an attractive method for combining networks of multi-output adaptive neural-fuzzy inference systems, which automatically estimate the number of clusters and the location of their clusters. In the reduction clustering algorithm, each sample point is seen as the center of the potential cluster. Using the reduction clustering algorithm, the data center, cluster determines the number of reduction centers to automatically generate membership functions, rules, as well as membership functions.

8. Results and Discussion

The grade of some elements was analyzed, and the statistical indices of these elements in heavy water and mineral sediments are shown in Tables 2 and 3, respectively.

The expectation of a geochemist working on a regional scale is to have normal log communities with positive skewness because these communities' high values with low frequencies can represent an economic potential.

The results of element analysis show that the rate of change of mercury (Ag) elements between 0.45 ppm and 0.45 ppm, aluminum (Al) between 60917 ppm and 37919 ppm, the amount of arsenic (As) between 14.40 ppm and 40.40 ppm, the amount of change in barium (Ba) is between 377 ppm and 251 ppm, the change in beryllium (Ba) is between 0.50 ppm and 0.00 ppm, and the change in calcium (Ca) is between 0.99632 ppm and 0.00 ppm. In the case of cadmium (Cd), it is observed that the amount of this element varies between 0.38 ppm and 0.24 ppm and cerium (Ce) between 49.00 ppm and 33.00. The range of changes in cobalt (Co) is between 17.00 ppm and 9.00 ppm, chromium (Cr) is between 8073 ppm and 00.00 ppm, and copper (Cu) is between 19.00 ppm and 41.00 ppm. Iron (Fe) between 00/38684 ppm and 00/20129 ppm, potassium (K) between ppm 00/17874-00/10865, lanthanum (La) between 00/26- 00/17, lithium (Li) between ppm 00/33-19.00, magnesium (Mg) between 0.0000/20000 ppm, manganese (Mn) between 0.800/814/009 ppm, molybdenum (Mo) between 0.65 ppm and 65.95 ppm, sodium (Na) between 14611-5855 ppm, nickel (Ni) between ppm 00/64-00/39 ppm, phosphorus (P) between 00/673-00/314 ppm, lead (Pb) between 00/40-00/15 ppm, sulfur (S) between 007-7654/006/006 ppm, antimony (Sb) between 1.29/1/79, scandium (Sc) between 10/11- 30/30 ppm, zinc (Zn) between ppm 00 /129-00/47 is variable. Strontium (Sr) between 0012-612/006 ppm, thorium (Th) between 11/10-20/7 ppm, titanium (Ti) between 4130-00/2289 ppm, uranium (U) between 30/0.00-16 ppm, vanadium (V) varies between 541.00/121.00 ppm, yttrium (Y) varies between 10.00-100.00 ppm, ytterbium (Yb) varies between 1.00/1/50 ppm, and zirconium (Zr) varies between 35.00/66-00 ppm.

Examination of skewness and elongation values of raw data of different elements showed that the highest skewness and elongation were related to sulfur (S) with values of 10.379 and 110.752, respectively. Also the lowest values of skewness and elongation of raw data are related to the element beryllium (Be) and lanthanum (La) with values of -3.687 and -0.598, respectively.

Table 2. Results of some of elements analyzed in present study.

sample / elements	1	2	3	4	5	6	7
Ag (ppm)	0.22	0.27	0.26	0.26	0.29	0.23	0.26
Al (ppm)	41615	41398	43549	42098	38337	38368	40803
As (ppm)	10.1	13.5	9.9	8.9	10.2	7.2	7.7
Ba (ppm)	329	377	339	355	344	324	321
Be (ppm)	1.1	1	1.1	1	<1	1	1
Ca (ppm)	78806	82771	86391	88435	91647	80590	78333
Cd (ppm)	0.29	0.38	0.26	0.29	0.29	0.31	0.3
Ce (ppm)	45	47	45	43	44	39	37
Co (ppm)	13	17	14	12	14	10	9
Cr (ppm)	479	349	405	137	82	159	123
Cu (ppm)	27	26	22	21	21	22	22
Fe (ppm)	32710	27954	28537	22759	21682	25221	23402
K (ppm)	13007	12199	11157	12447	13156	14315	14529
La (ppm)	24	23	23	20	19	24	22
Li (ppm)	24	21	20	22	22	25	25
Mg (ppm)	14484	13780	13152	14076	13856	15166	14593
Mn (ppm)	716	668	726	560	538	596	556
Mo (ppm)	0.77	0.85	0.84	0.83	0.73	0.79	0.75
Na (ppm)	1169	11639	11179	10790	11194	10585	9827
Ni (ppm)	51	46	46	41	44	49	46
P (ppm)	390	391	378	390	392	465	445
Pb (ppm)	23	27	29	19	19	24	24
S (ppm)	248	271	252	244	230	254	310
Sb (ppm)	1.11	1.01	1.11	1.16	0.85	0.96	1.06
Sc (ppm)	8.4	7.6	7.5	6.6	6.7	7.8	7.4
Zn (ppm)	44	40	39	44	44	54	55

Table 3. Statistical indicators of the elements of studied area.

Statistical index / Elements	Maximum	Minimum	Arithmetic Average	Standard deviation	Skewness	Kurtosis
Ag (ppm)	0.45	0.19	0.26	0.038	0.851	1.563
Al (ppm)	60917	37919	46273.9560	4002.2524	0.837	0.913
As (ppm)	14.40	6.40	8.9200	1.05	1.163	5.475
Ba (ppm)	377	251	313.5640	1.23	-0.500	1.140
Be (ppm)	1.50	0.00	1.09	0.22	-3.687	16.487
Ca (ppm)	99632	0.00	81601.74	24235.65596	-2.869	7.050
Cd (ppm)	0.38	0.24	0.29	0.019	0.464	1.453
Ce (ppm)	49.00	33.00	40.62	2.95	0.332	-0.140
Co (ppm)	17.00	9.00	11.42	1.05	0.999	3.794
Cr (ppm)	1073.00	80.00	180.78	91.94	4.608	36.563
Cu (ppm)	41.00	19.00	24.80	2.92	1.708	5.065
Fe (ppm)	38684.00	20129.00	25262.59	2026.09	1.732	8.625
K (ppm)	17874.00	10865.00	13775.37	1177.55	0.665	0.816
La (ppm)	26.00	17.00	21.32	1.66	0.136	-0.598
Li (ppm)	33.00	19.00	24.60	2.34	0.606	0.866
Mg (ppm)	20000.00	0.00	13822.86	7388.24	-1.277	-0.208
Mn (ppm)	814.00	509.00	600.63	55.36	1.501	2.409
Mo (ppm)	0.95	0.65	0.7678	0.05056	0.357	0.428
Na (ppm)	0.5855	14611	11123.1920	1413.0089	-0.584	2.063
Ni (ppm)	64.00	39.00	53.50	4.80	-0.365	-0.081
P (ppm)	673.00	314.00	439.13	42.14	0.765	3.464
Pb (ppm)	40.00	15.00	20.53	2.46	2.389	15.356
S (ppm)	7654.00	176.00	341.36	668.82	10.379	110.752
Sb (ppm)	1.29	0.79	0.98	0.08	0.541	0.734
Sc (ppm)	10.10	6.30	7.97	0.58	0.255	0.258
Zn (ppm)	129.00	47.00	62.71	8.24	3.183	14.923
Sr (ppm)	612.00	204.00	301.25	51.81	0.076	0.656
Th (ppm)	11.10	7.20	8.94	0.55	0.975	2.869
Ti (ppm)	4130.00	2289.00	2857.94	261.96	-0.819	1.597
U (ppm)	16.30	0.00	8.83	3.15	1.960	10.176
V (ppm)	121.00	54.00	70.37	7.46	0.003	-0.021
Y (ppm)	14.00	10.00	12.08	0.72	-0.046	0.221
Yb (ppm)	1.50	1.00	1.27	0.0779	3.384	21.542
Zr (ppm)	66.00	35.00	48.18	4.44	0.599	1.239

8.1. Prediction of lead and zinc elements using ANFIS model

After data processing, the correlation between the elements was evaluated using the correlation matrix prepared by the Pearson method in the SPSS software. According to the purpose of the study (prediction of the lead and zinc elements), we selected the elements that had the highest correlation with the lead and zinc elements as the input to the model. According to the correlation matrix, specified, the elements were found to be aluminum (Al), arsenic (As), barium (Ba), cadmium (Cd), cerium (Ce), cobalt (Co), chromium (Cr), copper (Cu), iron (Fe), lanthanum (La), manganese (Mn), molybdenum (Mo), sodium (Na), phosphorus (P), sulfur (S), scandium (Sc), thorium (Th), titanium (Ti), vanadium (V), yttrium (Y), yttrium (Yb), zinc (Zn) have the highest correlation with lead (Pb) compared to the other available elements. It was also found that the elements aluminum (Al), arsenic (As), barium (Ba), beryllium (Be), cadmium (Cd), cerium (Ce), cobalt (Co), chromium (Cr), copper (Cu), iron (Fe), potassium (K), lanthanum (La), lithium (Li), manganese (Mn), nickel (Ni), phosphorus (P), lead (Pb), scandium (Sc), thorium (Th), titanium (Ti), vanadium (V), yttrium (Y), yttrium (Yb) have the highest correlation with zinc (Zn) compared to the other available elements. Some results of the correlation matrix between the elements are given in Table 4. As shown in the correlation table, a good correlation is observed between the metal elements and the lead and zinc deposits, which can be an indication of the possible mineralization of lead and zinc in the carbonate type. The total number of geo-chemical data was 250, of which 70% of the data (175 data) were randomly selected as the training data and 30% of the data (75 data) as the test data.

Table 4. Some results of correlation matrix between analyzed elements

	Ag	Al	As	Ba	Be	Ca	Cd	Ce	Co	Cr	Cu	Fe	K
Ag	1	-0.046	-0.004	-0.123	0.061	0.038	0.021	0.030	0.047	0.022	0.044	0.057	0.059
Al	-0.046	1	0.374**	0.248**	**0.534	-0.081	0.048	0.409**	0.471**	-0.174**	0.358**	0.337**	0.676**
As	-0.004	0.374**	1	0.102	0.227**	-0.007	0.037	0.340**	0.506**	0.285**	0.246**	0.462**	0.266**
Ba	-0.123	0.248**	0.102	1	0.170**	0.109	0.477**	0.223**	0.104	0.284**	0.266**	0.252**	0.364**
Be	0.061	0.534**	0.227**	0.170**	1	0.244**	0.042	0.391**	0.309**	-0.213**	0.299**	0.275**	0.666**
Ca	0.038	-0.081	-0.007	0.109	0.244**	1	0.080	-0.003	-0.004	-0.074	0.059	0.013	0.104
Cd	0.021	0.048	0.037	0.223**	0.042	0.080	1	0.010	0.131*	0.103	0.115	0.114	-0.040
Ce	0.030	0.409**	0.340**	0.104	0.391**	-0.003	0.010	1	0.622**	0.231**	0.215**	0.637**	0.628**
Co	0.047	0.471**	0.506**	0.284**	0.309**	-0.004	1.31*	0.622**	1	0.541**	0.363**	0.885**	0.396**
Cr	0.022	-0.174**	0.285**	0.266**	-0.213**	-0.074	0.103	0.231**	0.541**	1	0.066	0.676**	-0.321**
Cu	0.044	0.358**	0.246**	0.252**	0.299**	0.059	0.115	0.215**	0.363**	0.066	1	0.344**	0.240**
Fe	0.057	0.337**	0.462**	0.364**	0.275**	0.013	0.114	0.637**	0.885**	0.676**	0.344**	1	0.317**
K	0.059	0.676**	0.266**	-0.012	0.666**	0.104	-0.040	0.628**	0.396**	-0.321**	0.240**	0.317**	1

8. 1.1. Data standardization

For the data to enter the adaptive neural-fuzzy inference system, it is necessary for the range of data changes to be similar to each other, which is called data standardization. Data standardization for logging into the adaptive neural-fuzzy inference system was also performed by Equation (3), which places the range of inputs in the range (-1.1).

$$p_n = 2\frac{p - p_{min}}{p_{max} - p_{min}} - 1 \quad (3)$$

wherein:

p_n : Standardized parameter;
p : True parameter;
p_{max} : Maximum real parameter;
p_{min} : Minimum real parameters [26, 27].

8.1.2. Model performance evaluation criteria

In order to evaluate the performance of the model, two indicators were used, the relationships of which are as follows:

$$R^2 = 1 - \frac{\sum_{i=1}^{n}(y_i - y_i')^2}{\sum_{i=1}^{n} y_i^2 - \frac{\sum_{i=1}^{n} y_i'^2}{n}} \quad (4)$$

$$MSE = \frac{1}{n}\sum_{i=1}^{n}(y_i - y_i')^2 \quad (5)$$

where:

y_i : Measured value and
y_i' : Predicted value.

The criterion R^2 indicates the correspondence between the measured and predicted values, which in the best case will be 1 and in the worst case - 1.

The MSE criteria also indicate an error between the measured and predicted values, and the lower the value, the more reliable the model performance.

8.1.3. Results obtained from ANFIS-SCM model

In this research work, the training and testing of the ANFIS-SCM model for the dataset were performed. The results obtained from the model are shown in Tables 5 and 6. As it can be seen in these tables, the ANFIS-SCM method is associated with high a reliability and accuracy in predicting the grade of the lead and zinc elements.

Figures 3 and 6 show the correlation between the measured and predicted values in the training and test dataset for the ANFIS-SCM model. In addition, the comparison between the measured and predicted values of Pb and Zn by ANFIS-SCM in the test and training stages is shown in Figures 4, 5, 7, and 8, which are due to correlation. The above is matched. The results obtained indicate that the ANFIS-SCM model has a high capability in estimating the lead and zinc elements using a set of input elements, and can be used optimally for other projects with similar conditions.

Table 5. Comparison between results of ANFIS-SCM model for training and test dataset (Pb).

Data collection		R^2	MSE
Pb	Train	0.9899	0.00045
(ANFIS-SCM)	Test	0.8399	0.0039

Table 6. Comparison between results of the ANFIS-SCM model for training and test dataset (Zn).

Data collection		R^2	MSE
Zn	Train	0.989	0.00042
(ANFIS-SCM)	Test	0.8607	0.00884

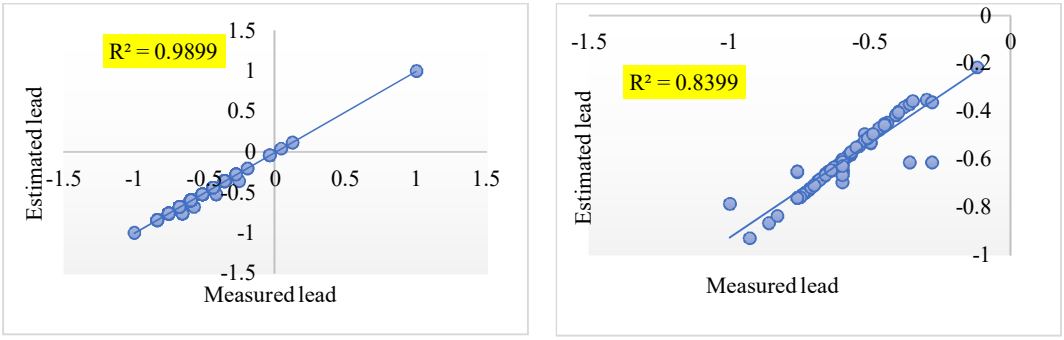

(a) (b)

Figure 4. Correlation between measured and predicted values in training dataset (A), test (B) (ANFIS-SCM) (Pb).

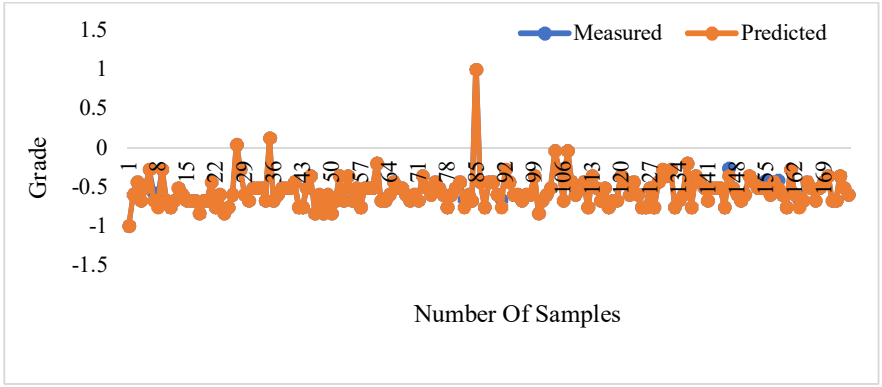

Figure 5. Graph of measured and predicted values in training dataset (ANFIS-SCM) (Pb).

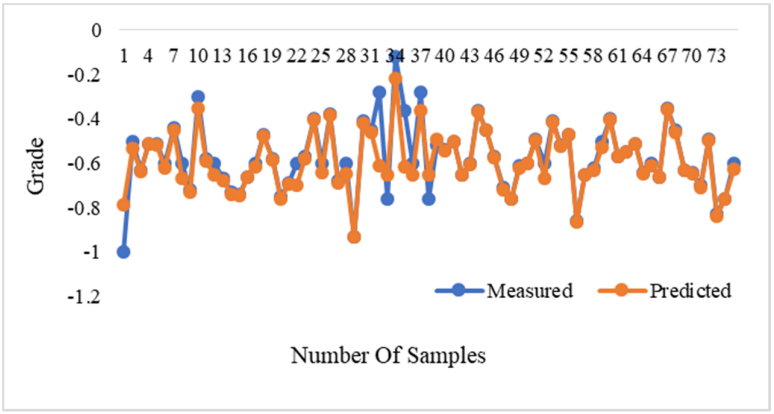

Figure 6. Graph of measured and predicted values in test dataset (ANFIS-SCM) (Pb).

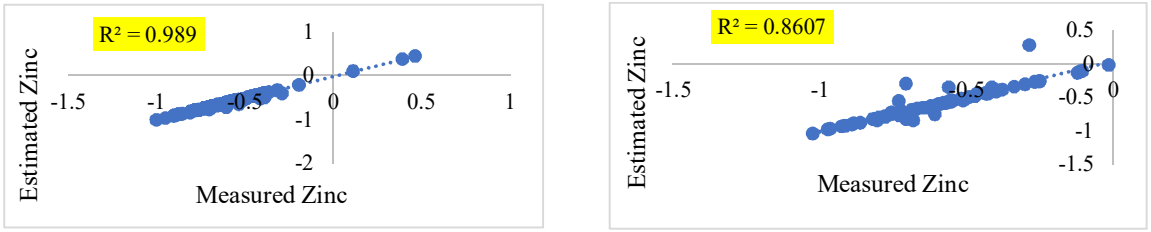

(a) **(b)**

Figure 7. Correlation between measured and predicted values in training dataset (A), test (B) (ANFIS-SCM) (Zn).

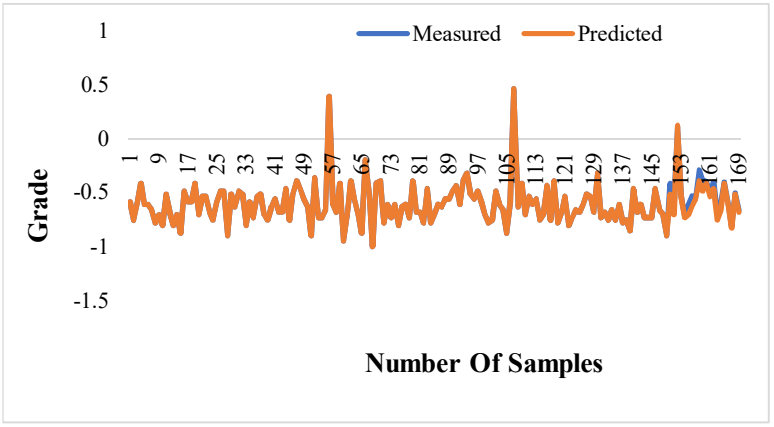

Figure 8. Graph of measured and predicted values in training dataset (ANFIS-SCM) (Zn).

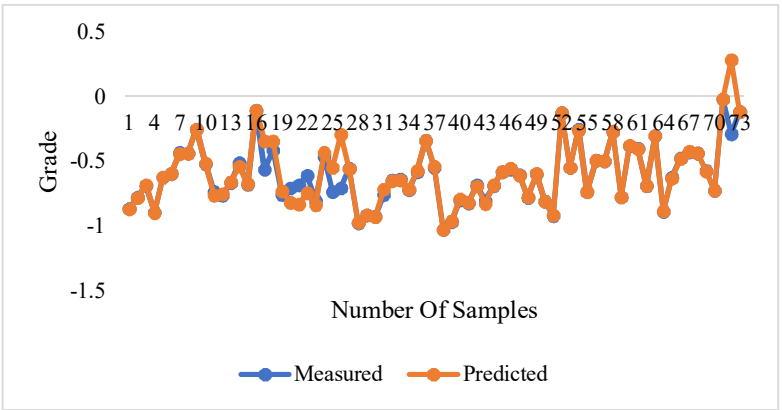

Figure 9. Graph of measured and predicted values in test dataset (ANFIS-SCM) (Zn).

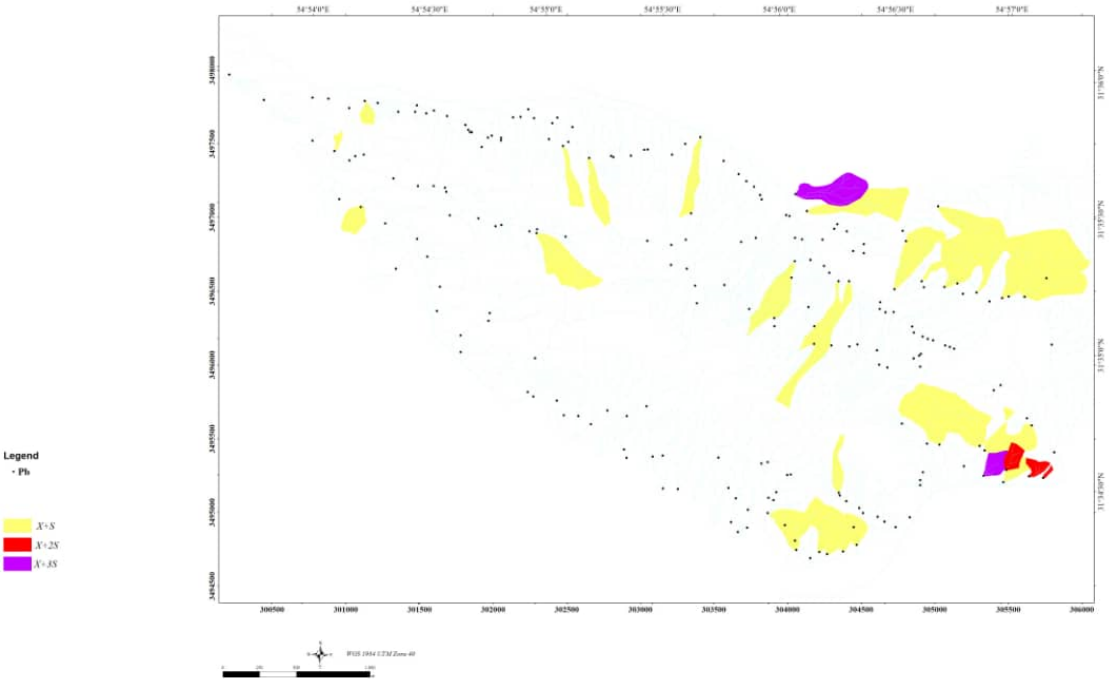

Figure 10. Map of lead element anomalies using stream sediment data in studied area.

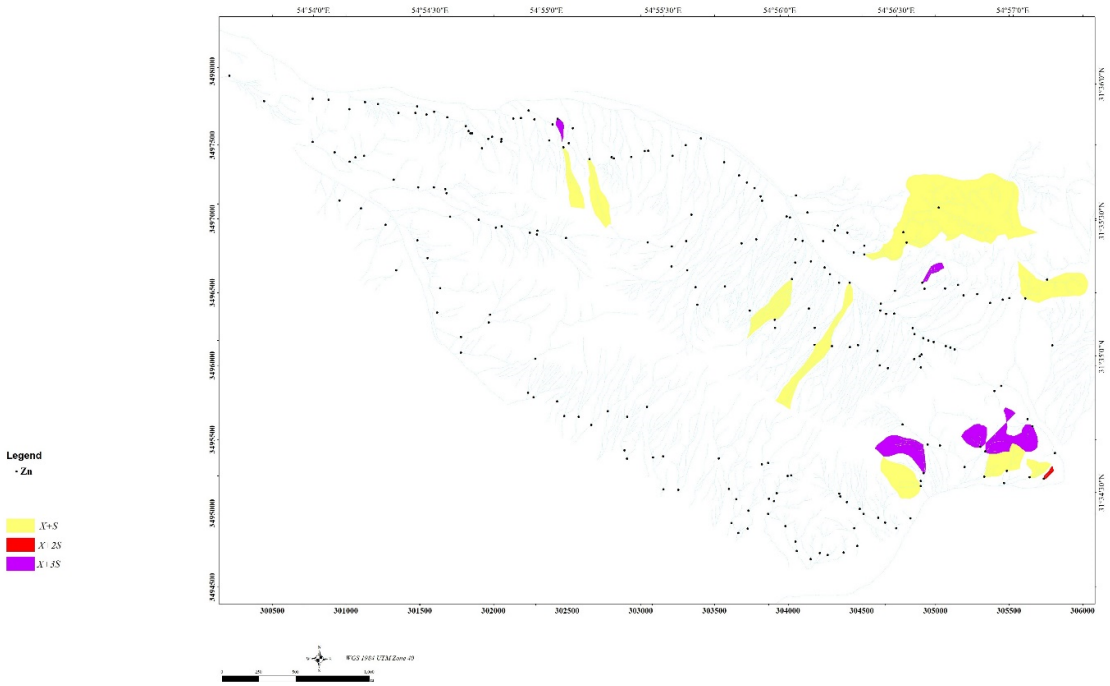

Figure 11. Map of zinc element anomalies using stream sediment data in studied area.

9. Conclusions

Based on the results of data analysis, pre-processing, and preparation of the correlation table between elements using correlation matrix that was prepared in SPSS software, and Pearson method, after standardization, the data was entered into the MATLAB environment, and the grade of the lead and zinc elements was predicted using the ANFIS-SCM method. While 70% of the data (175 samples) for the training dataset and 30% of the data (75 samples) for the test dataset were randomly selected, for the ANFIS-SCM model training dataset, for each one of the elements, the desired values of R2, MSE, were obtained as follows: lead (R2 = 0.989, MSE = 0.00045), zinc (R2 = 0.989,

MSE = 0.00042), as well as for the ANFIS model test dataset. The SCM Lead values (R2 = 0.8999, MSE = 0.0039), zinc (R2 = 0.8607, MSE = 0.884) were obtained. Using the results obtained from this model, it was found that the grade of the estimated elements in the studied area had a good accuracy and a high correlation with the measured values. As a result, the ANFIS-SCM intelligent method is a useful and accurate method for estimating the lead and zinc elements.

References

[1]. Bashkin, V. (2006). Modern biogeochemistry: Second Edition, Environmental Risk Assessment. Published by Springer, 3300 AA Dordrecht, The Netherlands, P.O. Box 17.

[2]. Bazdar, H. Fattahi, H., and Ghadim, F. (2015). Hybrid ANN with Invasive Weed Optimization Algorithm, a New Technique for Prediction of Gold and Silver in Zarshuran Gold Deposit, Iran. MSc Thesis, Arak University of Technology, Arak, Iran, 120 pp.

[3]. Skabar, A. (2003). Mineral potential mapping using feed-forward neural networks. Neural Networks, Proceedings of the International Joint Conference, 1814-1819.

[4]. Fung, CC. Iyer, V. Brown, W., and Wong, KW. (2005). Comparing the performance of different neural network architectures for the prediction of mineral prospectivity. Machine Learning and Cybernetics, Proceedings of 2005 International Conference, 394-398.

[5]. Leite, EP., and de Souza Filho, CR. (2009). Probabilistic neural networks were applied to the mineral potential mapping for platinum group elements in the Serra Leste region, Carajás Mineral Province, Brazil. Computers and Geosciences, 35(3), 675-687.

[6]. Wang, G. Zhang, S. Yan, C. Song, Y. Sun, Y. Li, D., and Xu, F. (2011). Mineral potential targeting and resource assessment based on 3D geological modeling in Luanchuan region, China. Computers and Geosciences, 37(12), 1976-1988.

[7]. Twarakavi, NK. Misra, D., and Bandopadhyay, S. (2006). Prediction of arsenic in bedrock-derived stream sediments at a gold mine site under conditions of sparse data. Natural Resources Research, 15(1), 15-26.

[8]. Abedi, M. Norouzi, GH., and Bahroudi, A. (2012). Support vector machine for multiclassification of mineral prospective areas. Computers & Geosciences, 83, 35-45.

[9]. Knox-Robinson, C. (2000). Vectorial fuzzy logic: a novel technique for enhanced mineral prospectivity mapping, concerning the orogenic gold mineralization potential of the Kalgoorlie Terrane, Western Australia, Australian Journal of Earth Sciences, Vol. 47, No. 5, pp. 929-941.

[10]. Abedi, M. Torabi, S., and Norouzi, G. (2013). Application of the fuzzy AHP method to integrate geophysical data in a prospect scale, a case study: Seridune copper deposit. Bollettino di Geofisica Teorica ed Applicata, 54(2), 145-164.

[11]. Tahmasebi, P. Hezarkhani, A. (2012). A hybrid neural networks-fuzzy logic-genetic algorithm for grade estimation. Computers and Geosciences, 42, 18-27.

[12]. Ziaii, M. Abedi, A., and Ziaii, M. (2007). Prediction of hidden ore bodies by new integrated computational model in marginal Lut region in east of Iran. Proc. Exploration, 957-961.

[13]. Renguang, Z. Jian, W., and Bojun, Y. (2021). Visualization and interpretation of geochemical exploration data using GIS and machine learning methods. Applied Geochemistry, volume 134.

[14]. Tahmooresi, M. Babaei, B., and Dehghan, S. (2021). Intelligent geochemical exploration modeling using multiclass support vector machine and integration with a continuous genetic algorithm in Gonabad region, Khorasan Razavi, Iran. Arabian Journal of Geosciences, volume 14, Article number: 1012.

[15]. Renguang, Z. Jian, W. Yihui, X., and Ziye, W. (2021). The processing methods of geochemical exploration data: past, present, and future. Applied Geochemistry, volume 132.

[16]. Guopeng, W. Guoxiong, Ch. Qiuming, Ch. Zhenjie, Z., and Jie, Y. (2021). Unsupervised Machine Learning for Lithological Mapping Using Geochemical Data in Covered Areas of Jining, China. Natural Resources Research, volume 30, pages1053–1068.

[17]. Bao-yi, Z. Man-yi, L. Wei-xia, L. Zheng-wen, J. Umair, K. Li-fang, W., and Fan-yun, W. (2021). Machine learning strategies for lithostratigraphic classification based on geochemical sampling data: A case study in area of Chahanwusu River, Qinghai Province, China. Journal of Central South University, volume 28, pages 1422–1447.

[18]. Ghadiyanloo, M. Alimoradi, A., and Yousefi, M. (2021). Recognizing Porphyry Copper Mineralization Targets in Chahar-Gonbad Area of Kerman Province Using Extreme Learning Intelligent Method. Journal of Mineral Resources Engineering (JMRE), volume 7, Issue 1 - Serial Number 23, Pages 39-61.

[19]. Nabavi, MH. (1976). An Introduction to Geology of Iran, Geological Survey of Iran.

[20]. Srinivasan, K. Fisher, D. (1995). Machine Learning Approaches to Estimating Software Development Effort. IEEE Transactions on Software Engineering, 21(2), 126–137.

[21]. Jang, JSR. Sun, CT. and Mizutani, E. (1997). Neuro-Fuzzy and Soft Computing, A Computational Approach to Learning and Machine Intelligence. Prentice-Hall, 640p.

[22]. Kosko, B. (1992). Neural Networks and Fuzzy Systems. A Dynamical Approach to Machine Intelligence, Prentice-Hall, Englewood Cliffs, NJ, 449p.

[23]. Nava, P. and Taylor, J. (1996). The Optimization of Neural Network Performance through Incorporation of Fuzzy Theory. In: 11th Conference on Systems Engineering, 897-901.

[24]. MATLAB user's guide. (2006). Fuzzy logic Toolbox, by math works Inc.

[25]. Chiu, SL. (1994). Fuzzy model identification based on cluster estimation. Journal of intelligent and Fuzzy Systems, 2(3), 267-278.

[26]. Gholami, R. Moradzadeh, A. Maleki, S. Amiri, S., and Hanachi, J. (2014). Applications of artificial intelligence methods in prediction of permeability in hydrocarbon reservoirs. J Pet Sci Eng, 122, 643-56.

[27]. Jayalakshmi, T. and Santhakumaran, A. (2011). Statistical normalization and backpropagation for classification. Int J Comput Theory Eng, 3(1), 1793-8201.

تخمین عیار عناصر سرب و روی با بهره‌گیری از روش سیستم استنتاج عصبی- فازی تطبیقی (مطالعه موردی: منطقه گرده کوه، شمال یزد)

شاهو رضائی*، علی امامعلی‌پور

بخش مهندسی معدن، دانشگاه ارومیه، ارومیه، ایران

ارسال ۲۰۲۲/۰۱/۰۲ پذیرش: ۲۰۲۲/۰۶/۱۹

* نویسنده مسئول مکاتبات: shahou44@gmail.com

چکیده:

به دلیل دشوار بودن اندازه‌گیری دقیق پارامترها و مرزبندی آن‌ها، در چند سال اخیر سعی بر آن شده است که با استفاده از مدل‌سازی، وقایع طبیعی برای بررسی بهتر، ساده گردند. مدل‌سازی با روش‌های هوشمند از جمله روش‌های جدیدی است که در سالیان اخیر در این حوزه مورد توجه قرار گرفته است. در این مطالعه، روش هوشمند سیستم استنتاج عصبی- فازی تطبیقی (ANFIS)، در پیش‌بینی عناصر سرب و روی واقع در منطقه گرده کوه، شمال یزد، مورد استفاده قرار گرفته است. آمارهای توصیفی داده‌ها و ماتریس همبستگی عناصر مورد مطالعه با استفاده از نرم افزار SPSS بدست آمد. جهت انجام این تحقیق، داده‌ها پس از استاندارد-سازی، وارد محیط متلب شده و با استفاده از روش ANFIS-SCM، عناصر سرب و روی پیش‌بینی گردید. در این روش ۷۰ درصد داده‌ها (۱۷۵ نمونه) برای مجموعه داده آموزش و ۳۰ درصد داده‌ها (۷۵ نمونه) برای مجموعه داده آزمون به طور تصادفی انتخاب شدند. با استفاده از نتایج به دست آمده از این مدل، مشخص شد که عیار عناصر تخمین زده شده در محدوده‌ی مورد بررسی از دقتی بسیار خوب و همبستگی بالایی نسبت به عیار عناصر آنالیز شده برخوردار بوده است. در نتیجه روش هوشمند ANFIS-SCM روشی مفید و دقیق جهت تخمین عناصر سرب و روی می‌باشد.

کلمات کلیدی: علوم زمین، ANFIS-SCM، عناصر سرب و روی، شمال یزد.